Supporting Information

Site−specific Photo–crosslinking in a Double Crossover DNA tile Facilitated by Squaraine Dye Aggregates: Advancing Thermally Stable and Uniform DNA Nanostructures

Table of Contents

Supporting Information 1: *Tile sequences and nanostructures*

The DNA oligomer sequences were purchased from IDT (Integrated DNA Technologies, Inc.). A custom dichloroindolenine squaraine dye was obtained from SETA BioMedicals (Urbana–Champaign, IL). Labeling of oligomers with dichloroindolenine squaraine via NHS–ester and subsequent purification by dual HPLC was performed at IDT (Integrated DNA Technologies, Inc.).

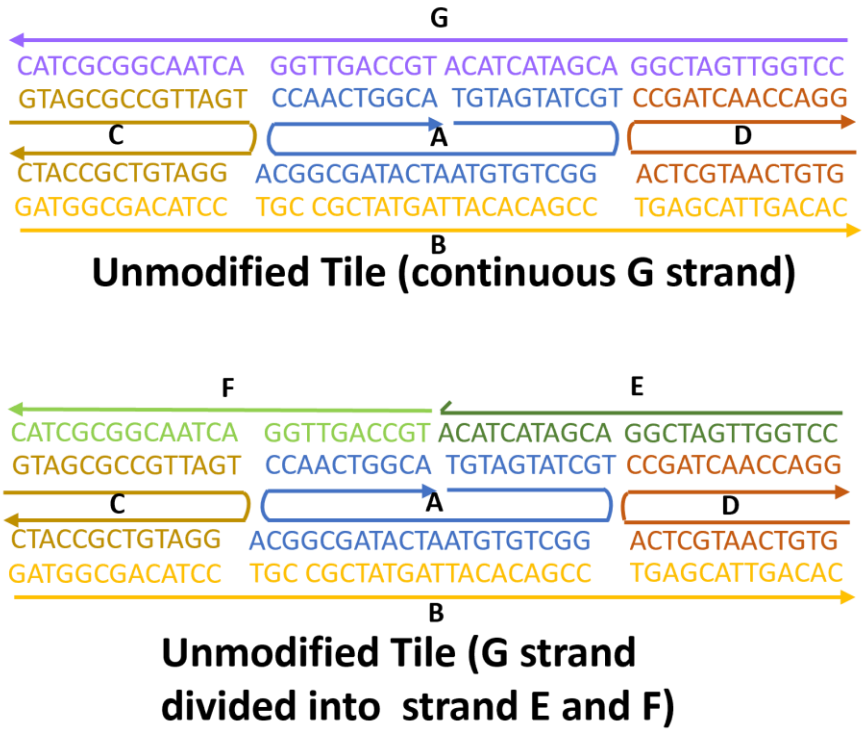

Figure S1. DNA nanostructure designs of unmodified tiles, composed of single−stranded DNAs (ssDNAs) labeled A, B, C, D, E, F, and G. In unmodified Tile, no thymine is labeled with SQ dye.

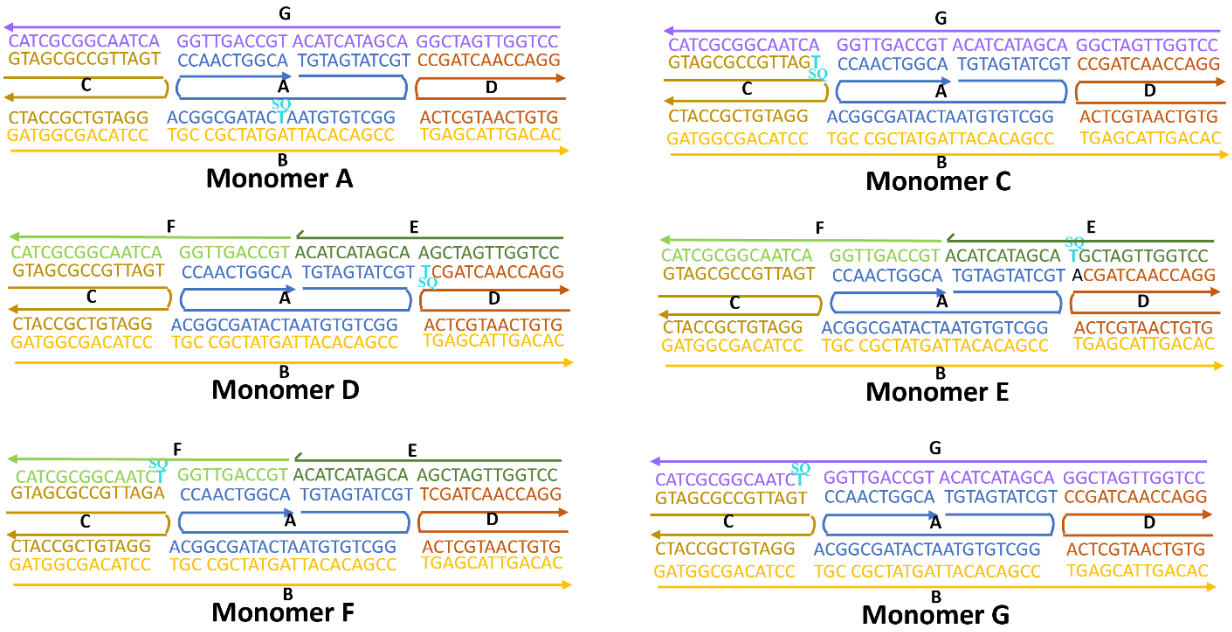

Figure S2. DNA tile designs of modified SQ-monomer. In the modified monomer, thymine is labeled with only one SQ dye on the strand A/C/D/E/F/F.

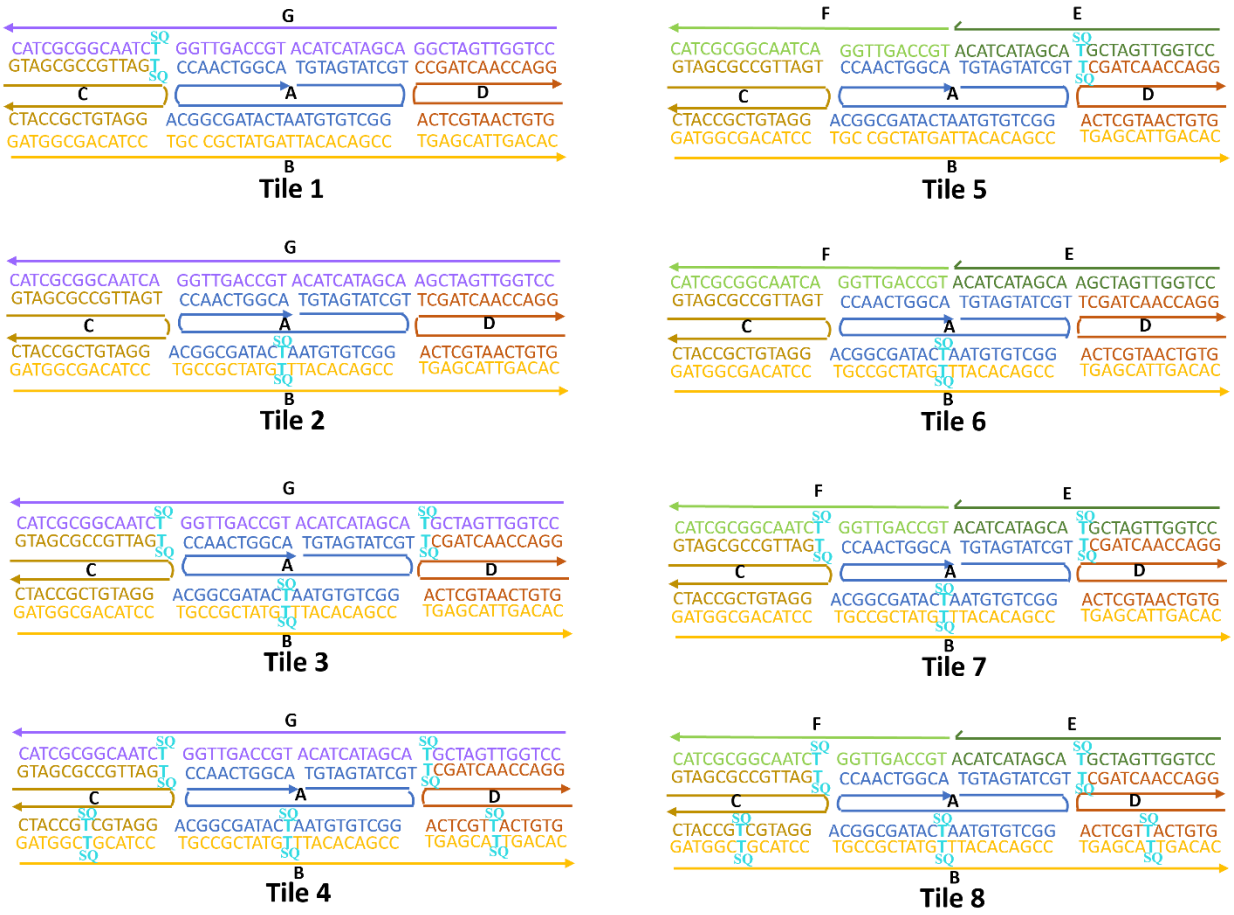

Figure S3. DNA tile designs of modified SQ-dimer. In the modified dimer, opposite thymines are labeled with SQ dye.

Supporting Information 3: *Electrophoretic analysis of crosslinked DNA constructs*

Raw gels (i. e. without contrast and brightness adjustments) were analyzed in ImageJ 1.53e.[1] Photocrosslinking yield was calculated as follows:

$$\text{Photocrosslinking Yield [\%]} = \frac{A_R}{A_{NR}} \times 100$$

where A_R is the area under the peak corresponding to the band of crosslinked DNA; A_{NR} is the area (29967.2 and 29856.1) under the peak corresponding to band of the non-irradiated DNA. The photocrosslinking yields are summarized in **Tables S1 and S2.**

Table S1: Yield of crosslinked T5D5 analyzed by ImageJ.

Irradiation Time (Hour)	Peak	Peak Area(A_R)	A_R/A_{NR}, %
0.5	1	3741.7	12
1	2	5245.5	17
1.5	3	6732.9	22
2	4	8793.4	29
2.5	5	9910.1	33
3	6	11243.9	37
4	7	13177.3	43
5	8	16619.58	55

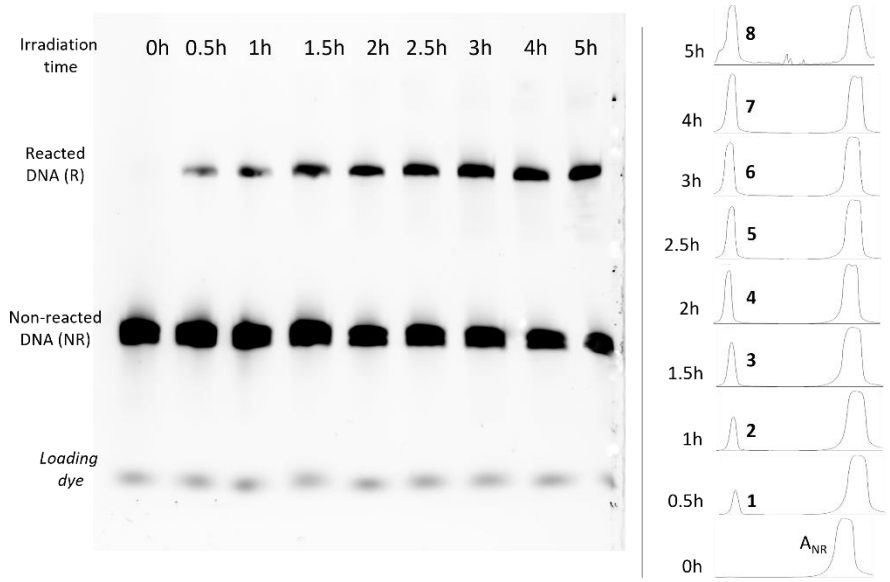

Figure S4. Fluorescent images (ex. 632 nm: em. 691 nm) of 12% denaturing PAGE, 1.5 mm–thick, of T5D5.The electrophoresis was performed at 57 °C in 1× TBE running buffer. Quantification of the raw gel in ImageJ showing lane selections and corresponding peak areas.

Table S2: Yield of crosslinked T10D5 analyzed by ImageJ.

Irradiation Time (Hour)	Peak	Peak Area(A_R)	A_R/A_{NR}, %
0.5	1	2123.6	7
1	2	2825.4	9
1.5	3	6871.8	23

2	4	7603.1	25
2.5	5	10210.1	34
3	6	11243.9	39
4	7	12454.7	41
5	8	12578.4	42

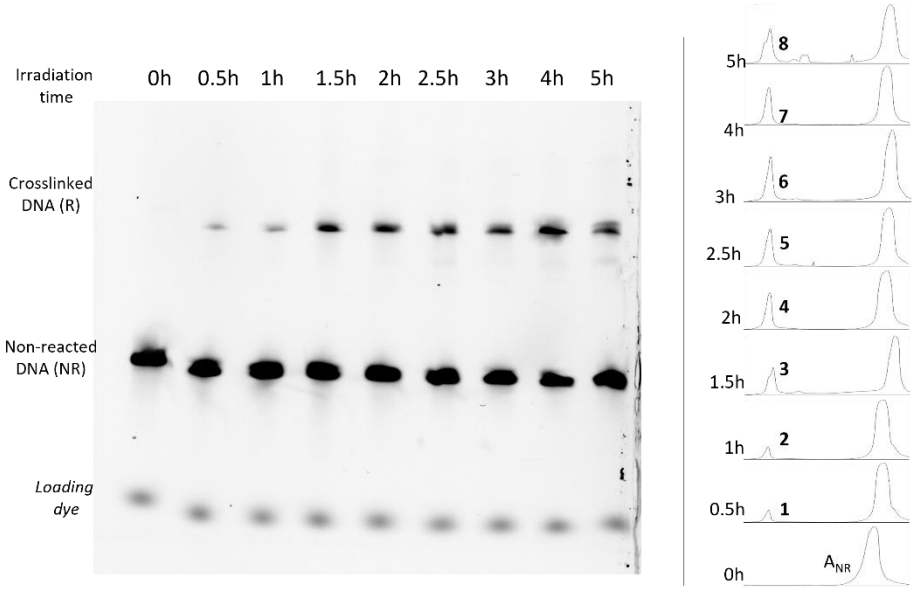

Figure S5. Fluorescent images (ex. 632 nm: em. 691 nm) of 12% denaturing PAGE, 1.5 mm–thick, of T10D5.The electrophoresis was performed at 57 °C in 1× TBE running buffer. Quantification of the raw gel in ImageJ showing lane selections and corresponding peak areas.

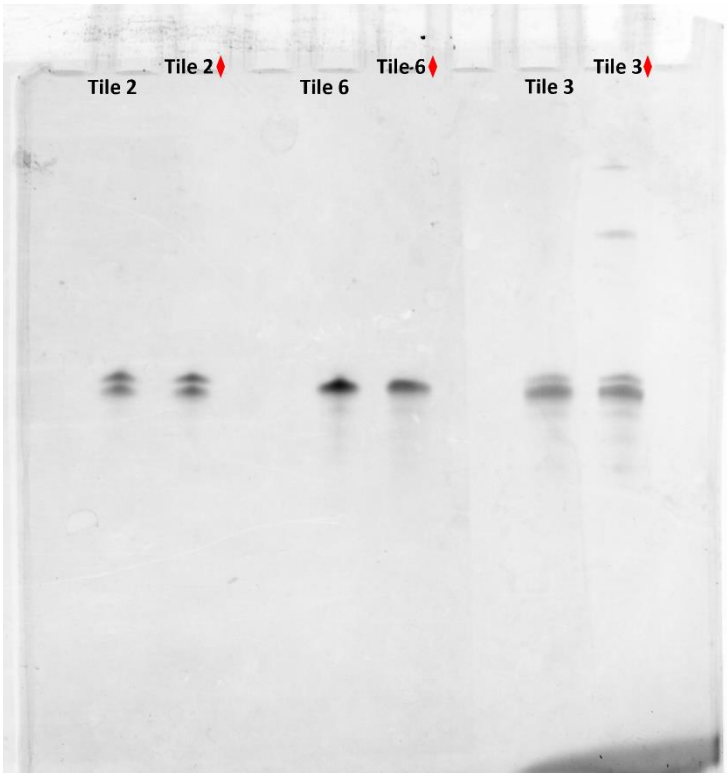

Figure S6. Fluorescent images (ex. 632 nm: em. 691 nm) of 12% denaturing PAGE, 1.5 mm–thick. The electrophoresis was performed at 57 °C in 1× TBE running buffer. Red diamond symbol indicating irradiated samples.

Supporting Information 3: *Purification through denaturing gel electrophoresis*

The photo crosslinked tile samples were purified by 12% denaturing PAGE gel. DNA templating SQ–dimer (20 uM, 50 uL) in 1×TBE, 15mM $MgCl_2$, was irradiated for 4 hours at room temperature at 310 nm wavelength. DNA samples were mixed with equal volume loading buffer (formamide: 100×TBE, 9:1 v/v) and heated at 95 °C for 4 min to denature the DNA prior loading on gel. Samples were run on PAGE gel was run at 350 V applied voltage at 56 °C constant temperature for 25 min in running buffer 1×TBE. The bands of crosslinked products were excised separately and crushed the bands carefully in Freeze 'N Squeeze spin columns (Bio–Rad, Hercules, CA) and placed at –20 °C for 15 min. Samples were spanned down at 13000 g for 3 min to collect the

filtrate. 250 uL of 1×TBE, 15mM $MgCl_2$ was added to the tube and incubated overnight at 4°C. All samples were spun at 13,000g for 3 min and filtrates were transferred to the Amicon centrifugal tube for enrichment and buffer exchange. Crosslinked samples were placed in 10 kD MWCO Amicon tube, followed by three rounds of ultrafiltration with added fresh buffer every time. The samples were recovered by inverting the inner chamber in a collecting tube and spinning at 2,000 rpm for 2 min.

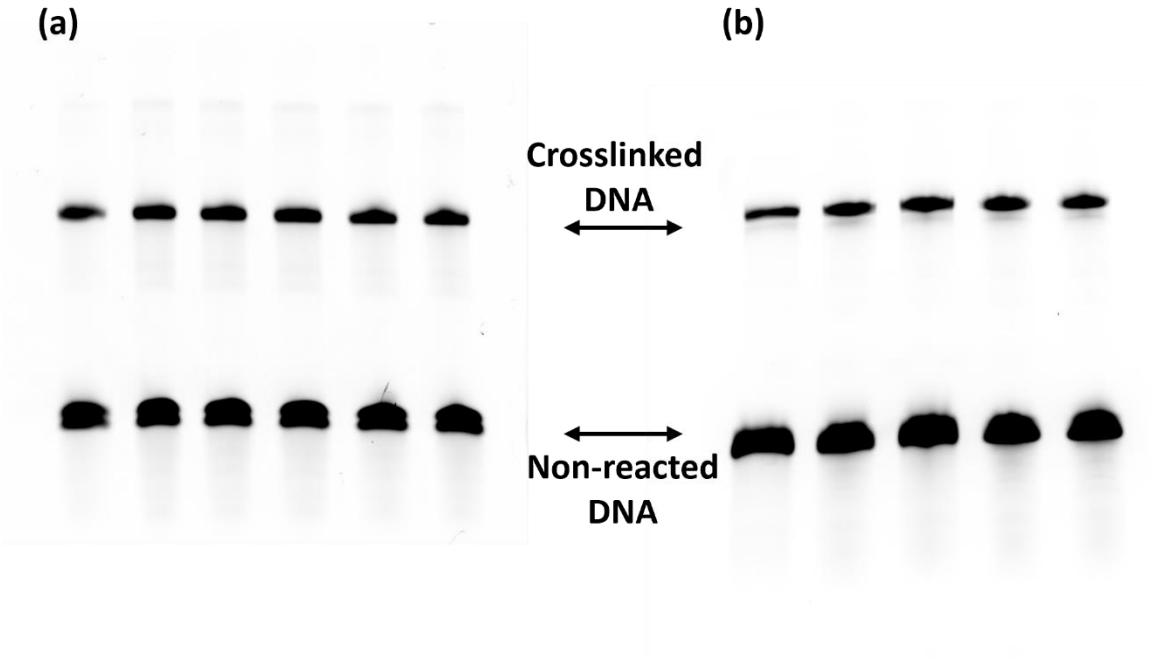

Figure S7. Fluorescent images (ex. 632 nm: em. 691 nm) of 12% denaturing PAGE, 1.5 mm–thick, of (a) Tile 4 and (b) Tile 8.The electrophoresis was performed at 57 °C in 1× TBE running buffer.

Supporting Information 4: *Spectral properties of SQ–labeled Tile constructs*

The absorption spectra of irradiated and non–irradiated constructs were recorded (Fig. S6–S8) in 1× TBE with 15 mM $MgCl_2$. All non-irradiated SQ–monomers showed electronic absorption spectra with a weak vibrionic shoulder characteristic for squaraine dye family. A strong and narrow low energy absorption band and a weak vibrionic component assigned as (0–0) and (0–1) transitions was observed in monomer spectra. Absorption maxima range about 645–647 nm for (0–0) transition, and approximately 598–600 nm for (0–1) transition. No significant spectral changes were noticed in the dimers compared to their corresponding non–irradiated constructs. Next, we characterized CD spectra to explore the aggregation behavior or the exciton chirality of the dye with the DNA connected by multiple number of SQ dyes. All dimer constructs showed a strong couplet at the 260–280 nm region representing a well–formed duplex DNA. No significant change was noticed after 4h of irradiation.

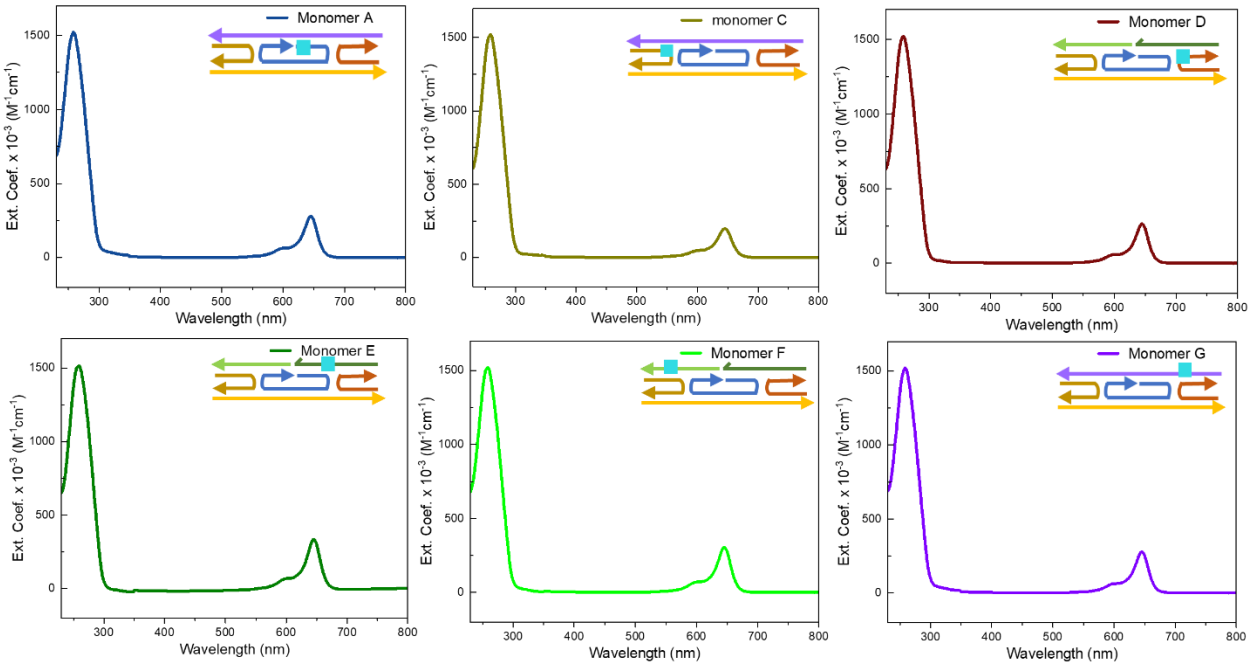

Figure S8. Acquired steady–state absorption spectra converted to extinction of squaraine–monomer constructs in 1× TBE, 15 mM $MgCl_2$ at room temperature The DNA–dye construct concentration was 1.5 μM.

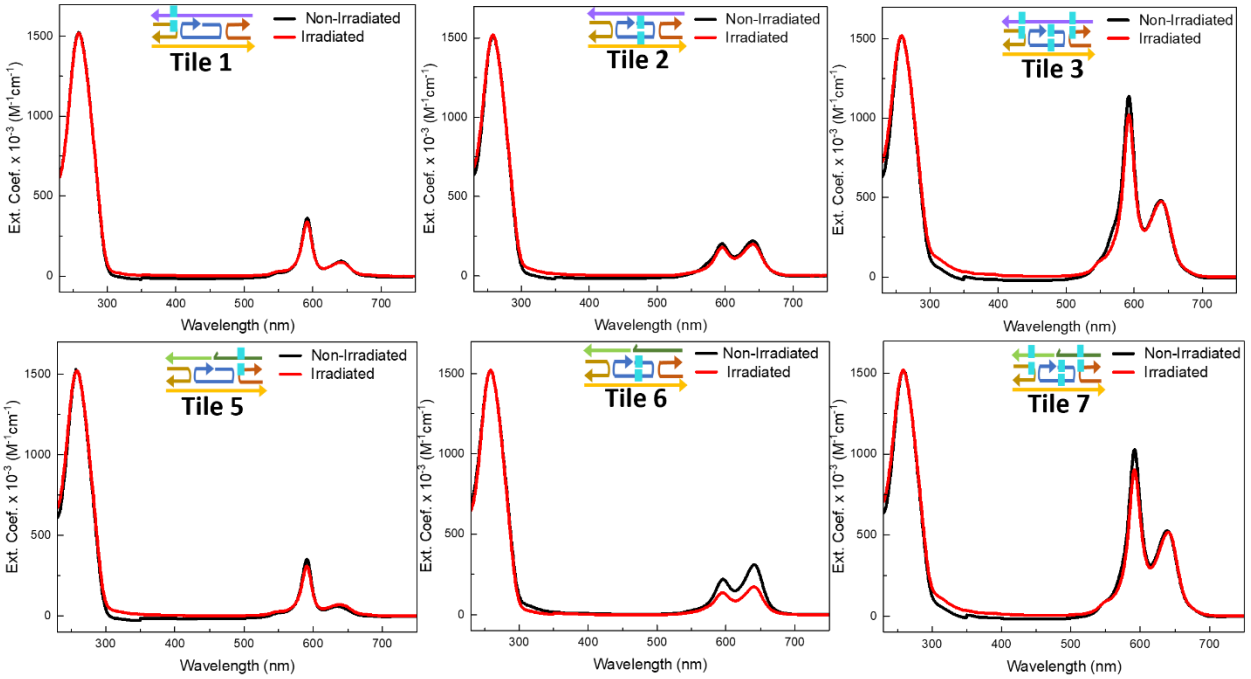

Figure S9. Acquired steady–state absorption spectra converted to extinction of squaraine–dimer constructs in 1× TBE, 15 mM $MgCl_2$ at room temperature The DNA–dye construct concentration was 1.5 μM.

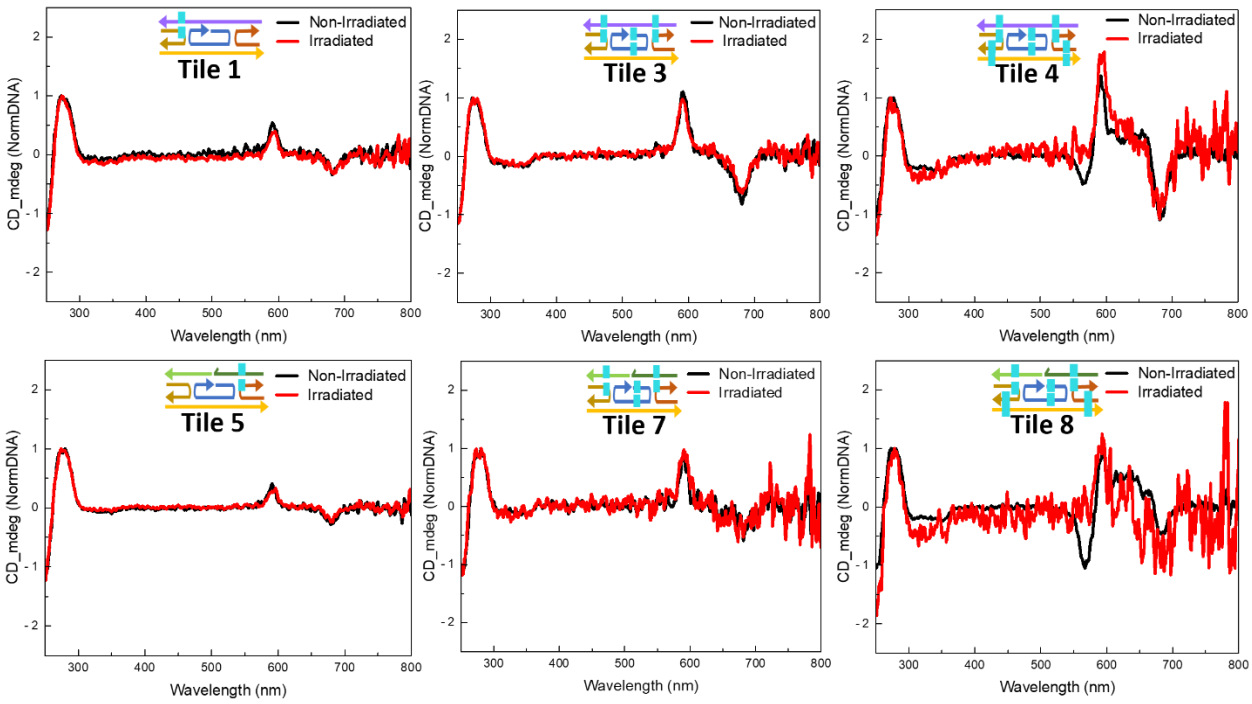

Figure S10. Full CD spectra of the constructs were recorded in 1× TBE, 15 mM $MgCl_2$ at room temperature. The DNA–dye construct concentration was 1.5 μM.

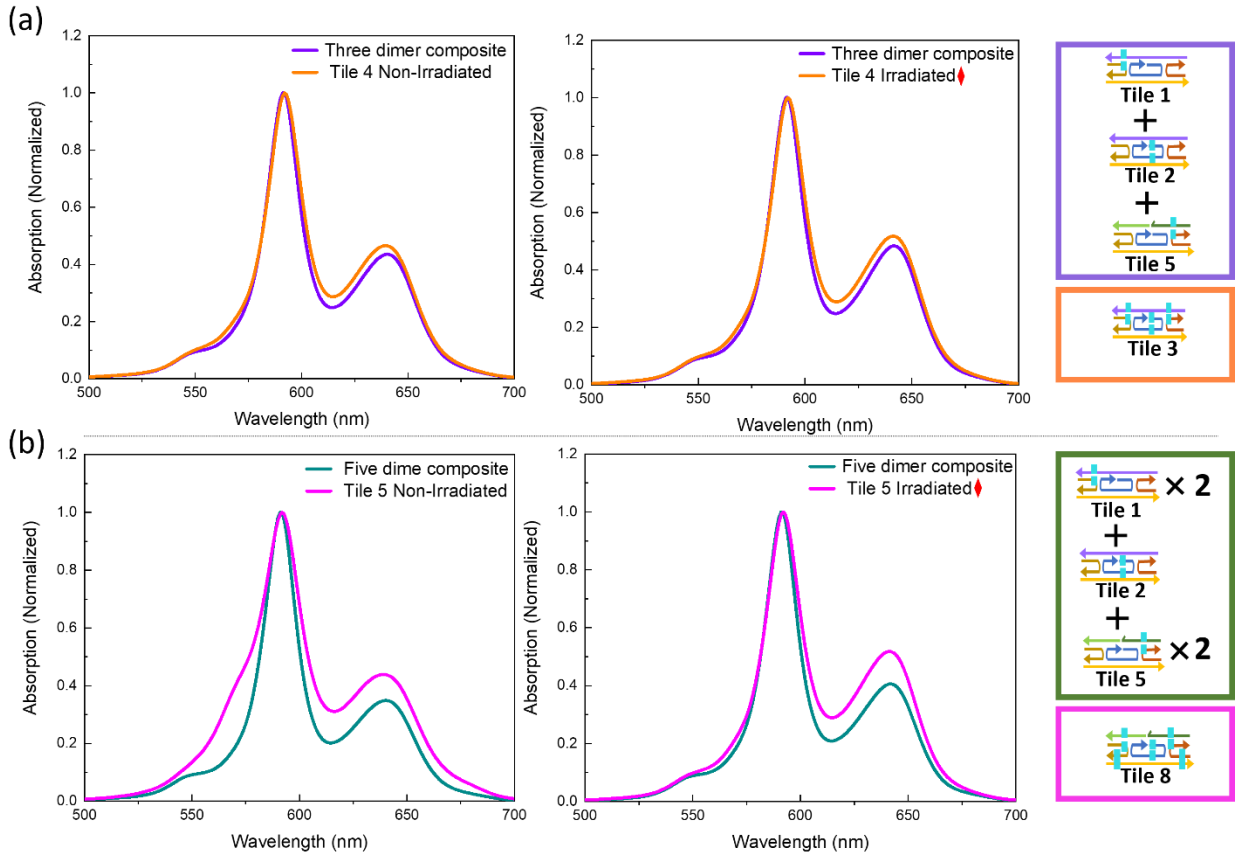

Figure S11. Acquired steady-state absorption spectral analysis of squaraine–dimer constructs confirming the proper formation of multi-dimer DNA constructs. Linear combinations of individual dimer spectra were compared to the absorption spectra of Tile 3 and Tile 8, verifying the presence of three (a) and five-dimer pairs (b), respectively. The analysis also demonstrates that these multi-dimer tiles can support up to five strongly- coupled dimers without inducing inter-dimer aggregation. Red diamond symbol indicating irradiated samples.

Supporting Information 5: To assess the impact of crosslinking on aggregate optical properties of the templated dye aggregates, we began by characterizing representative dimers using our in-house KRM Model Simulation Tool based on the work of Kühn, Renger, and May2,3. Briefly, the model employs a Holstein-like Frenkel Hamiltonian4 that is populated with experimentally derived parameters to calculate absorption and circular dichroism spectra from a given arrangement of transition dipole moments (TDMs) using an extended dipole approximation. The calculated spectra are compared with experimental spectra. An iterative stochastic approach is used to determine the TDM geometry that produces the best match to experimental data.

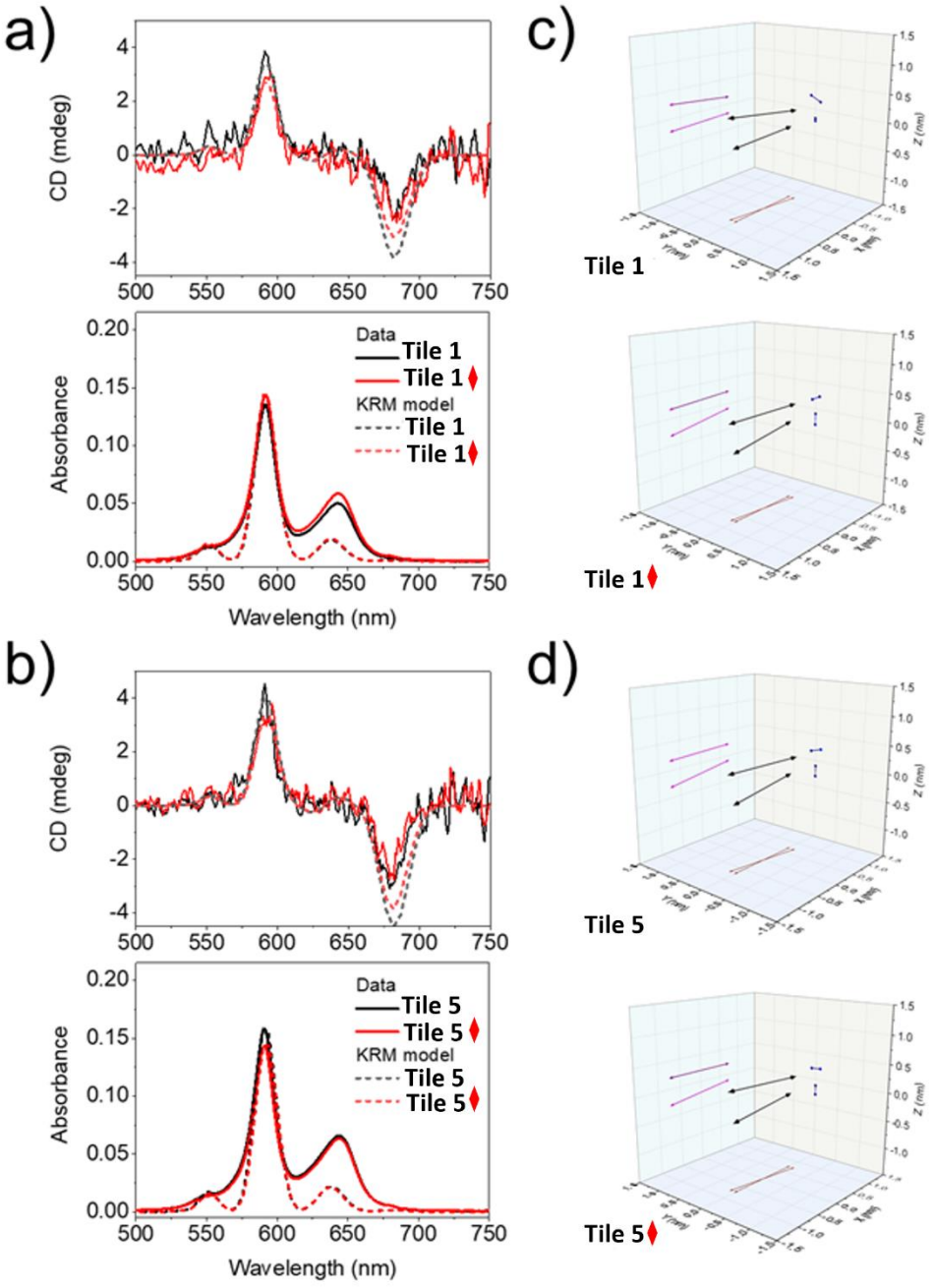

Figure S12. Panels (a) and (b) show experimental (solid) and KRM-modeled (dashed) the circular dichroism and absorbance spectra for non-irradiated (black) and irradiated (red) samples of Tile 1 and Tile 5, respectively. Panels (c) and (d) show KRM-derived 3D models of the transition dipole arrangements that give rise to the modeled spectra. Red diamond symbol indicating irradiated samples.

References:

(1) Schneider, C. A.; Rasband, W. S.; Eliceiri, K. W. *NIH Image to ImageJ: 25 Years of Image Analysis HHS Public Access*; 2012; Vol. 9.

(2) Kühn, O.; Renger, T.; May, V. Theory of Exciton-Vibrational Dynamics in Molecular Dimers. *Chemical Physics* **1996**, *204* (1), 99–114. https://doi.org/10.1016/0301-0104(95)00448-3.

(3) Roy, S. K.; Mass, O. A.; Kellis, D. L.; Wilson, C. K.; Hall, J. A.; Yurke, B.; Knowlton, W. B. Exciton Delocalization and Scaffold Stability in Bridged Nucleotide-Substituted, DNA Duplex-Templated Cyanine Aggregates. *Journal of Physical Chemistry B* **2021**, *125* (50), 13670–13684. https://doi.org/10.1021/acs.jpcb.1c07602.

(4) Abramavicius, D.; Mukamel, S. Exciton Delocalization and Transport in Photosystem I of Cyanobacteria Synechococcus Elongates: Simulation Study of Coherent Two-Dimensional Optical Signals. *Journal of Physical Chemistry B* **2009**, *113* (17), 6097–6108. https://doi.org/10.1021/jp811339p.